Supplemental Figures and Legends for "The capabilities and limitations of conductance-based compartmental neuron models with reduced branched or unbranched morphologies and active dendrites"

Submission to: Journal of Computational Neuroscience

Eric B. Hendrickson[1,2], Jeremy R. Edgerton[2], Dieter Jaeger[2]

1. Biomedical Engineering Dept, Georgia Inst of Tech, 313 Ferst Dr. Atlanta, GA, 30332

2. Biology Dept, Emory University, 1510 Clifton Rd NE. Atlanta, GA, 30322

Contact information:

Dieter Jaeger

Department of Biology, Emory University

1510 Clifton Rd. NE, Atlanta, GA, 30322

djaeger@emory.edu

Supplemental Figure S1

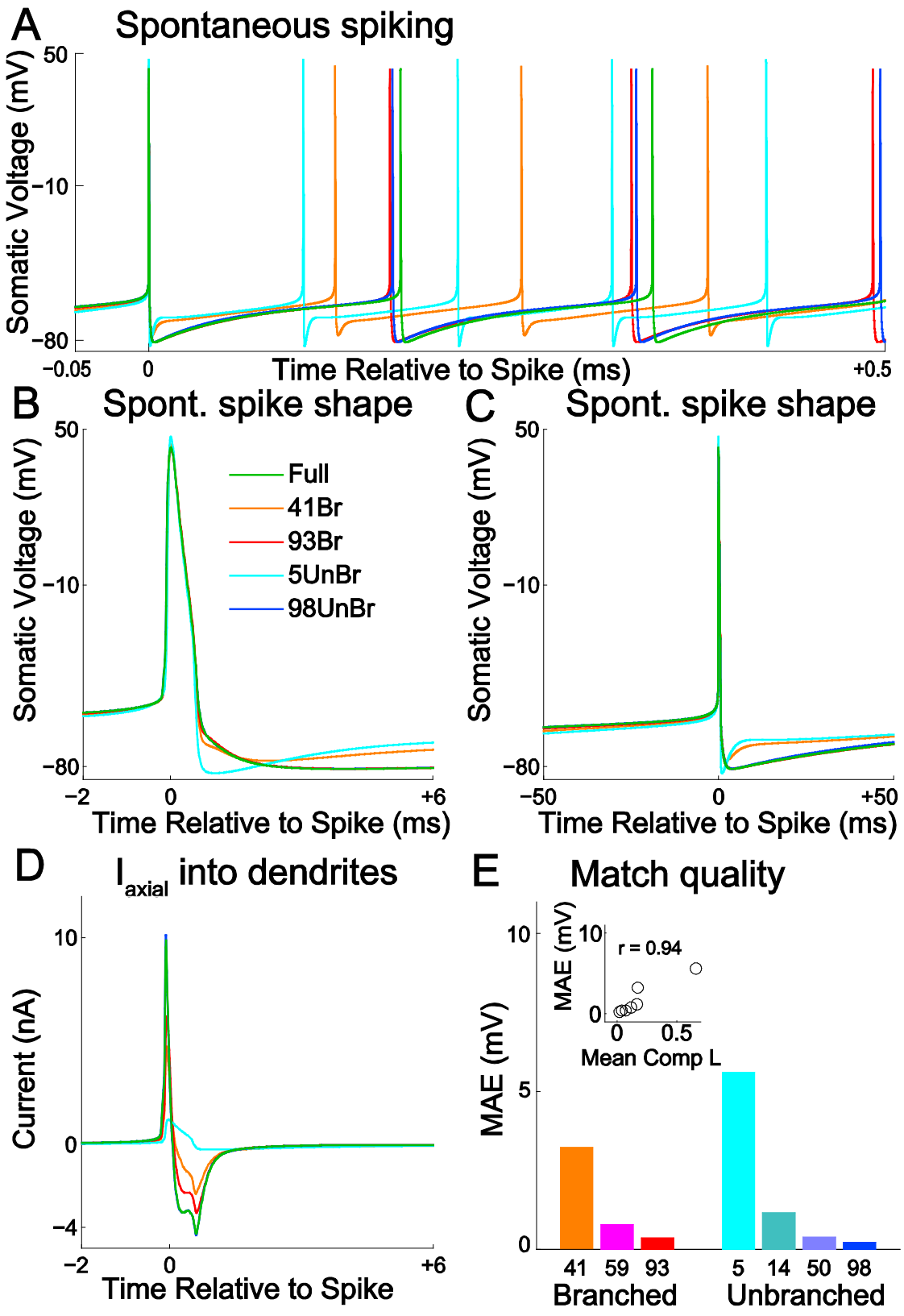

Supplemental Figure S1: High dendritic gNa density did not affect the ability of the reduced models to match the full model's spike shape. ***A,*** Spontaneous spiking is shown for the full and reduced models. ***B,*** Note that both the 93comp branched and 98comp unbranched models provide close qualitative matches to the full model's spike shape, while the 5comp unbranched and 41comp branched models show mismatches starting with the fast AHP. ***C,*** Note the wider time window compared to that in ***B***. The 93comp and 98comp models again provided close qualitative matches to the full model's spike shape, while the 5comp and 41comp models did not. ***D,*** The differences in somatic spike shape between the models were due to differences in axial current flow. The large positive axial current flow out of the soma into the dendrites occurred during the somatic spike. The subsequent negative axial current flow denotes the flow of current from the dendrites back into the soma following the spike. ***E,*** The 'match' to the full model spontaneous spike shape shown in ***B*** was calculated for each model as the MAE of the voltage traces from 2 ms before to 6 ms after the spike. Smaller MAEs represented closer matches. Spikes were aligned so that they crossed 0 mV at the same time.

Supplemental Figure S2:

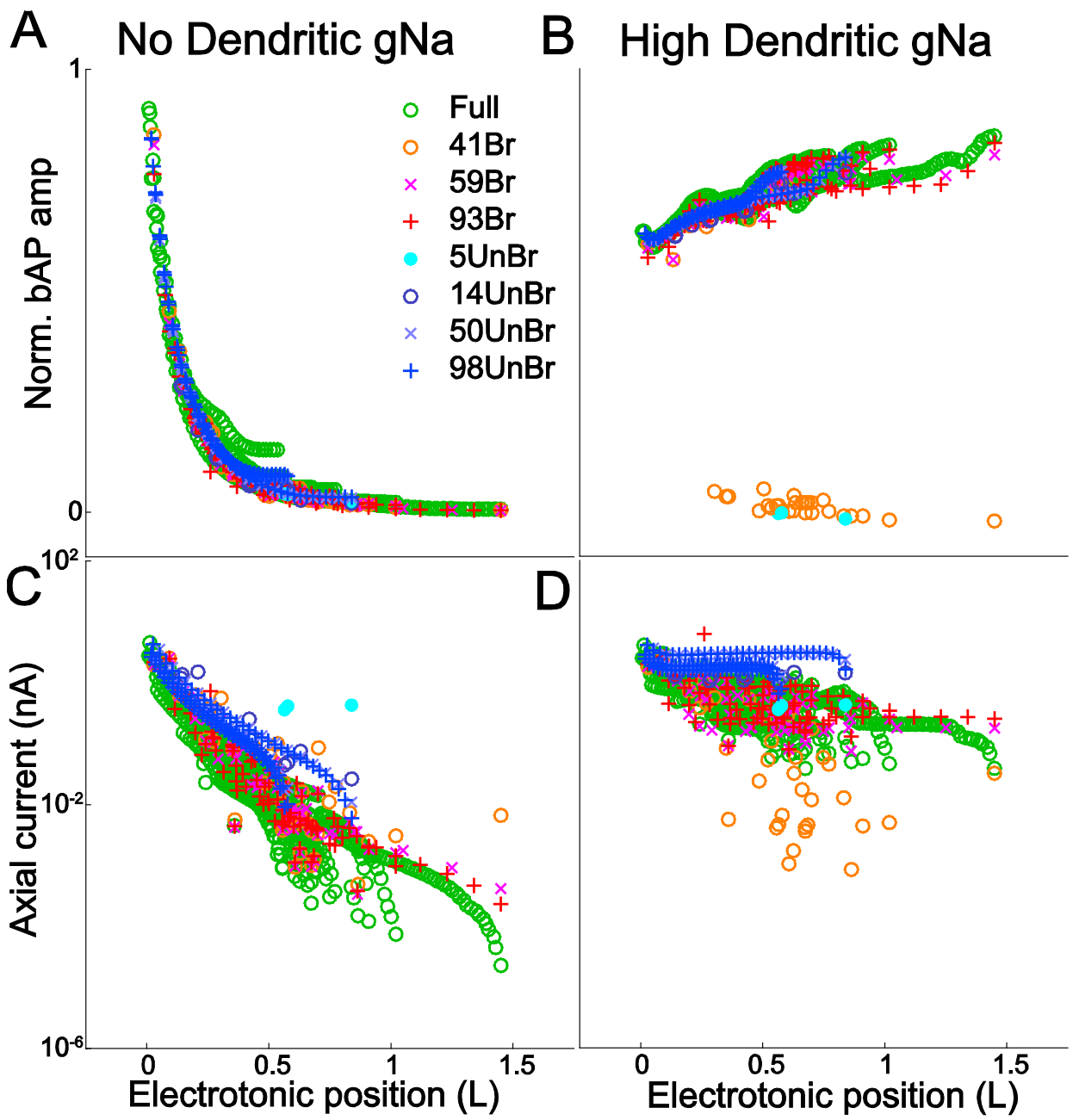

Supplemental Figure S2: bAP amplitudes were quite similar between most models with either no or high dendritic gNa density. All models were driven to fire at 75 Hz +- 0.1% with DC somatic injection. Under these conditions, all models were plotted together in the same panels because different models exhibited quite similar bAP amplitudes. ***A,*** The bAP amplitude in each compartment of each model was plotted against that compartment's electrotonic distance from the soma. With no dendritic gNa, bAP amplitude decayed with electrotonic distance at about the same rate in all the models. ***B,*** With high dendritic gNa, bAP amplitude slightly increased with electrotonic distance at about the same rate in all models. However, the bAP amplitude decayed sharply in the 5comp and 41comp models. ***C,*** The log of the maximum amount of axial current flowing into each compartment during a spike (referred to simply as axial current) was plotted against electrotonic distance from the soma. With no dendritic gNa, the axial current decayed with electrotonic distance at approximately the same rate in each model. ***D,*** With high dendritic gNa, axial currents decayed with electrotonic distance quite slowly due to successfully back propagating spikes in most of the models.

Supplemental Figure S3:

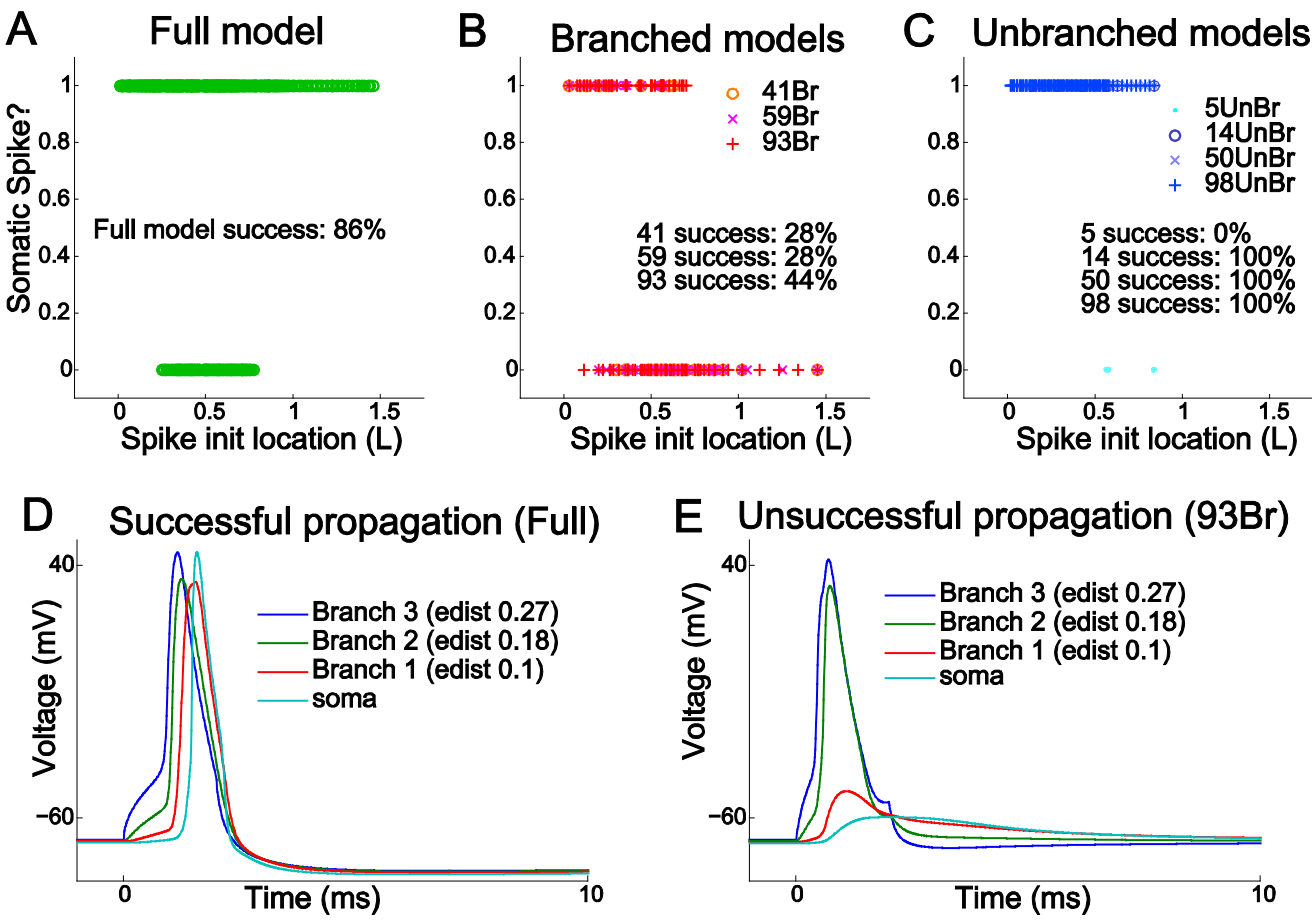

Supplemental Figure S3: In the models with high dendritic gNa, dendritically initiated spikes propagated to cause somatic spikes with success rates that varied by model type. To assess dendritic spike propagation to the soma, each model was prevented from firing spontaneously with -41 pA somatic DC injection. Dendritic spikes were initiated with brief (2 ms) but powerful (400 pA) current injections in each dendritic compartment of each model. Dendritically initiated spikes were considered to have successfully propagated to the soma if they caused the soma to spike. A, Dendritically initiated spikes propagated to the soma successfully from most (86.5%) dendritic initiation sites in the full model. B, In contrast to the full model, dendritically initiated spikes rarely propagated to the soma successfully in the branched reduced models. The branched reduced model with the highest success rate (93comp, 44.0%) had only about half the success rate of the full model. C, Also in contrast to the full model, dendritically initiated spikes always propagated to the soma in the divided unbranched reduced models, while they never did in the 5comp model. D-E, A comparison of dendritic spike propagation showed that the full model allowed dendritic spikes to propagate to the soma while the 93comp branched model did not, despite identical spike initiation locations in ‘Branch 3’.

Supplemental Figure S4:

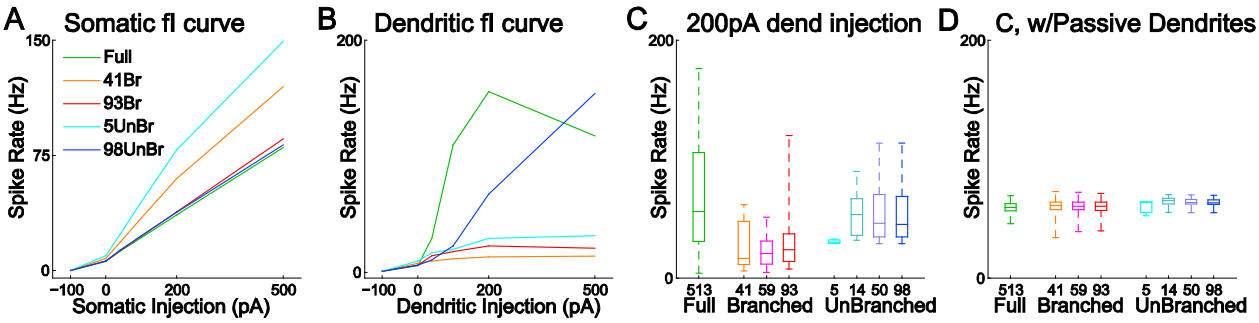

Supplemental Figure S4: Models with high dendritic gNa that allowed dendritic spike initiation still exhibited good matches to the full model's somatic fI curves but exhibited poor dendritic fI curve matches. DC injection amplitudes ranged from -100pA to +500pA to explore the full physiological range of model spike frequencies. ***A,*** The somatic fI curves plotted here were quite similar to those with medium dendritic gNa (Fig. 6*A*). ***B,*** The spike frequency of each model was plotted for each level of DC injection in the same dendritic compartments featured in Fig. 6*B*. In contrast to the somatic fI curves, the dendritic fI curves with high dendritic gNa were quite different from those with medium gNa (Fig. 6*B*). Note that the full and 98comp models fired many times faster than the 5comp, 41comp or 93comp models at most amplitudes of positive current injection. ***C,*** The spike frequency response was plotted for 200 pA DC injections in each compartment of each model. In contrast to the case with medium dendritic gNa (Fig. 6*C*), the branched reduced models exhibited slower median firing rates than the full model. While the unbranched reduced models possessed comparable median firing rates to those of the full model, the full model's wide range of firing rates was not matched by any reduced model. ***D,*** Same as ***C***, but with all dendritic channels removed. Data are identical to those shown in Fig. 6*D*, but are reproduced here for easier comparison. Note the close match between the responses of all the models.

Supplemental Figure S5:

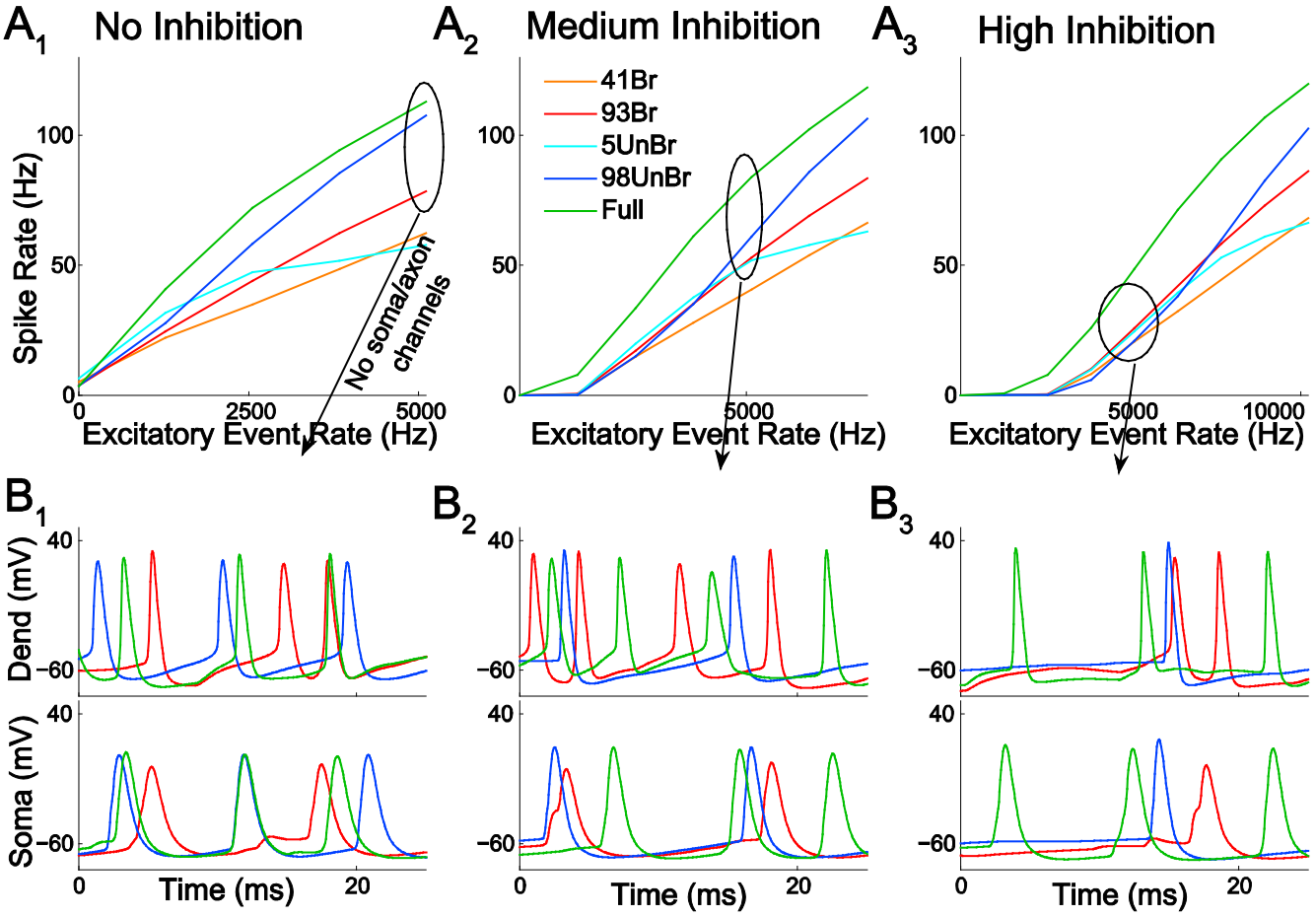

Supplemental Figure S5: The full model's fF curves with high dendritic gNa could not be matched by any reduced model. This figure is similar to Fig. 8 except that the density of dendritic sodium conductance was increased to 800 S/m^2 to allow dendritic spike initiation. ***A*$_{1\text{-}3}$,** In contrast to the case with medium dendritic gNa, the full model had steeper fF curves than any reduced model at every combination of inhibition and excitation tested. ***B*$_{1\text{-}3}$,** Somatic and axonal conductances were removed to prevent somatic spike generation. The steeper fF curves of the full model were due to its high ability to generate dendritic spikes given its large dendritic voltage fluctuations in response to synaptic input (e.g. Fig. 8*C*) coupled with its high ability to propagate dendritic spikes to the soma (e.g. Supplemental Fig. S3). Note that most of the spikes observed in the example dendritic location propagated to the full model's soma, while many fewer dendritic spikes propagated to the soma in the 93comp branched model (see Supplemental Fig. S3). Further note that, in general, fewer dendritic spikes were initiated in the dendrites of the 98comp model due to lower dendritic voltage fluctuations (e.g. Fig. 8*C*).

Supplemental Tables and Legends:

Supplemental Table S1: voltage-dependent gates

Channel	Gate	Pwr	Min_{inf}	$V_{0.5inf}$ mV	K_{inf} mV	τ_{min} ms	τ_{max} ms	$V_{0.5\tau}$ mV	$K_{\tau1}$ mV	$K_{\tau2}$ mV
Na_F	m	3	0	-39	5	0.028	0.028	NA	NA	NA
Na_F	h	1	0	-48	-2.8	0.25	4	-43	10	-5
Na_F	s	1	0.15	-40	-5.4	10	1000	-40	18.3	-10
Na_P	m	3	0	-57.7	5.7	0.03	0.146	-42.6	14.4	-14.4
Na_P	h	1	0.154	-57	-4	10	17	-34	26	-31.9
Na_P	s	1	0	-10	-4.9					
K_V2	m	4	0	-33.2	9.1	0.1	30	-33.2	21.7	-13.9
K_V2	h	1	0.2	-20	-10	3400	3400	NA	NA	NA
K_V3	m	4	0	-26	7.8	0.1	14	-26	13	-12
K_V3	h	1	0.6	-20	-10	7	33	0	10	-10
K_V4_{fast}	m	4	0	-49	12.5	0.25	7	-49	29	-29
K_V4_{fast}	h	1	0	-83	-10	7	21	-83	10	-10
K_V4_{slow}	m	4	0	-49	12.5	0.25	7	-49	29	-29
K_V4_{slow}	h	1	0	-83	-10	50	121	-83	10	-10
KCNQ	m	4	0	-61	19.5	6.7	100	-61	35	-25
Ca_{HVA}	m	1	0	-20	7	0.2	0.2	-20	NA	NA
HCN_{fast}	m	1	0	-76.4	-3.3	0	3625	-76.4	6.56	-7.48
HCN_{slow}	m	1	0	-87.5	-4	0	6300	-87.5	8.9	-8.2

Channel	A_α mV^{-1} ms^{-1}	B_α ms^{-1}	K_α mV	A_β mV^{-1} ms^{-1}	B_β ms^{-1}	K_β mV
Na_P	-2.88 X 10^{-6}	-4.9 X 10^{-5}	4.63	6.94 X 10^{-6}	4.47 X 10^{-4}	-2.63

Supplemental Table S1: Voltage-dependent gates.

Steady-state equation for all voltage-dependent gates:

$$X_{inf}(V_m) = Min_{inf} + [(1 - Min_{inf}) / (1 + \exp ((V_{0.5inf} - V_m) / K_{inf})]$$

Standard kinetic equation:

$$\tau(V_m) = \tau_{min} + [(\tau_{max} - \tau_{min}) / (\exp ((V_{0.5\tau} - V_m) / K_{\tau 1}) + \exp ((V_{0.5\tau} - V_m) / K_{\tau 2}))]$$

Kinetics for Na_P slow inactivation (s) gate:

$$\alpha(V_m) = [(A_\alpha * V_m) + B_\alpha] / [1 - \exp ((V_m + (B_\alpha / A_\alpha)) / K_\alpha)]$$

$$\beta(V_m) = [(A_\beta * V_m) + B_\beta] / [1 - \exp ((V_m + (B_\beta / A_\beta)) / K_\beta)]$$

$$\tau(V_m) = 1 / (\alpha(V_m) + \beta(V_m))$$

For a more detailed description of the voltage dependent gates used in this study, see Gunay et al 2008.

Supplemental Table S2: calcium-dependent gate

Channel	Gate	Pwr	$[Ca^{2+}]_{Sat}$ (µM)	EC_{50} (µM)	$K_{\tau\text{-}Ca}$ (ms/µM)	Hill Coeff
SK_{Ca}	m	1	5	0.35	14.4	4.6

Supplemental Table S2: calcium-dependent gate

SK channel calcium dependence (n = the Hill Coefficient):

$X_{inf}([Ca^{2+}]) = [Ca^{2+}]^n / ([Ca^{2+}]^n + (EC_{50})^n)$

SK channel kinetics:

--for $[Ca^{2+}] < [Ca^{2+}]_{Sat}$, $\tau([Ca^{2+}]) = \tau_{max} - ([Ca^{2+}] * [(\tau_{max} - \tau_{min}) / K_{\tau\text{-}Ca}])$

--for $[Ca^{2+}] >= [Ca^{2+}]_{Sat}$, $\tau([Ca^{2+}]) = \tau_{min}$

Supplemental Table S3: Model conductance density parameter sets used in this study.

Conductance	Tuned Densities (S/m2)	RandSet1 (fast)	RandSet2 (slow)
NaF soma	2500	9955	2953
NaP soma	1	3.863	1.672
Kv2 soma	320	121.3	439.6
Kv3 soma	640	2281	277.1
Kv4fast soma (Kv4slow = 1.5*Kv4fast)	160	174.1	242.5
KCNQ soma	0.4	0.123	0.268
SK soma	50	29.68	56.16
CaHVA soma	2	5.982	5.132
HCNfast soma (HCNslow = 2.5*HCNfast)	0.2	0.506	0.144
NaF dend	0 / **40** / 800	10.07	18.66
NaP dend	0 / **1**	1.475	1.629
Kv2 dend	64	148.3	25.89
Kv3 dend	128	63.15	196.8
Kv4fast dend (Kv4slow = 1.5*Kv4fast)	160	47.79	186.3
KCNQ dend	0.4	0.207	0.43
SK dend	4	1.330	5.848
CaHVA dend	0.15	0.143	0.079
HCN dend	0.2	0.160	0.071
NaF axon	5000	3597	2990
NaP axon	40	116.9	10.76
Kv2 axon	640	513.5	1250
Kv3 axon	1280	703.0	2485
Kv4fast axon (Kv4slow = 1.5*Kv4fast)	1600	457.2	3761
KCNQ axon	0.4	0.184	0.104

Supplemental Table S3: Model conductance density parameter sets used in this study. The tuned parameter set was used in most figures. ‘RandSet1’ and ‘RandSet2’ were two of the randomly generated parameter sets used in Fig. 10. RandSet1 and RandSet2 were chosen to demonstrate mapping of reduced model parameter sets back to the full model because they respectively produced the fastest and slowest spiking with 500pA somatic current injection.

Supplemental Table S4: Comparison of match quality between models for 100 randomly generated parameter sets.

Measure	41Br vs 59Br	59Br vs 93Br	5UnBr vs 14UnBr	14UnBr vs 50UnBr	50UnBr vs 98UnBr	59Br vs 50UnBr	93Br vs 98UnBr
Spike shape MAEs	+0.85 mV (p = 6.5e-4)	+0.95 mV (p = 2.3e-6)	+4.3 mV (p = 1.1e-14)	+2.1 mV (p = 9.1e-16)	~~~ (p = 0.067)	+1.9 mV (p = 6.3e-15)	+1.0 mV (p = 5.7e-14)
Soma fI curve MAEs	~~~ (p = 0.0087)	+2.4 Hz (p = 1e-4)	+8.9 Hz (p = 6.8e-7)	+4.7 Hz (p = 2.2e-11)	~~~ (p = 0.053)	+2.9 Hz (p = 3.3e-7)	+1.1 Hz (p = 2.2e-4)
Dist fI curve MAEs	~~~ (p = 0.19)	+1.5 Hz (p = 5.6e-5)	~~~ (p = 0.025)	~~~ (p = 0.24)	~~~ (p = 0.87)	**-3.4 Hz** (p = 5.1e-6)	**-4.9 Hz** (p = 1.9e-11)

Supplemental Table S4: Comparison of match quality between models for 100 randomly generated parameter sets. For each cell, the median MAEs of the 100 randomly generated parameter sets were compared between the two models denoted in the column header using the Mann-Whitney U test with Bonferroni correction ($n = 21 \rightarrow \alpha = 0.05 / 21 = 0.0024$). If the comparison was significant ($p < \alpha$), we listed the value of the median MAE of the second model listed in the column header subtracted from that of the first. When this value was negative, we highlighted it with bold text. The first 5 columns show within reduced model type comparisons (branched vs branched and unbranched vs unbranched) while the last 2 columns show across reduced model type comparisons (branched vs unbranched) with similar numbers of compartments.